



**Michigan
Technological
University**

Michigan Technological University
Digital Commons @ Michigan Tech

Michigan Tech Publications

8-23-2019

Surface water microbial community response to the biocide 2-2-dibromo-3-nitrilopropionamide used in unconventional oil and gas extraction.

Maria Fernanda Campa
University of Tennessee, Knoxville

Stephen Techtmann
Michigan Technological University, smtechtm@mtu.edu

Mallory P Ladd
University of Tennessee, Knoxville

Jun Yan
Chinese Academy of Sciences

Megan Patterson
University of Tennessee, Knoxville

Follow this and additional works at: <https://digitalcommons.mtu.edu/michigantech-p>

 Part of the [Life Sciences Commons](#)

Recommended Citation

Campa, M., Techtmann, S., Ladd, M., Yan, J., Patterson, M., Garcia de Matos Amaral, A., & et. al. (2019). Surface water microbial community response to the biocide 2-2-dibromo-3-nitrilopropionamide used in unconventional oil and gas extraction.. *Applied and environmental microbiology*. <http://dx.doi.org/10.1128/AEM.01336-19>
Retrieved from: <https://digitalcommons.mtu.edu/michigantech-p/386>

Follow this and additional works at: <https://digitalcommons.mtu.edu/michigantech-p>

 Part of the [Life Sciences Commons](#)

Authors

Maria Fernanda Campa, Stephen Techtmann, Mallory P Ladd, Jun Yan, Megan Patterson, Amanda Garcia de Matos Amaral, and et. al.

1 **Surface water microbial community response to the biocide 2-2-dibromo-3-**
2 **nitrilopropionamide used in unconventional oil and gas extraction**

3
4 **Maria Fernanda Campa^{1,2}, Stephen M. Techtman³, Mallory P. Ladd^{1,4}, Jun Yan^{5,6}, Megan**
5 **Patterson⁶, Amanda Garcia de Matos Amaral⁶, Kimberly E. Carter⁷, Nikea Ulrich⁸,**
6 **Christopher Grant⁸, Robert L. Hettich^{1,4}, Regina Lamendella⁸, Terry Hazen^{*,1,2,6,7,9,10}.**

7
8 ¹ Bredezen Center for Interdisciplinary Research and Graduate Education, University of
9 Tennessee, Knoxville, TN.

10 ² Biosciences Division, Oak Ridge National Laboratory, Oak Ridge, TN.

11 ³ Department of Biological Sciences, Michigan Technological University, Houghton, MI

12 ⁴ Chemical Sciences Division, Oak Ridge National Laboratory, Oak Ridge, TN

13 ⁵ Key Laboratory of Pollution Ecology and Environmental Engineering, Institute of Applied
14 Ecology, Chinese Academy of Sciences, Shenyang, Liaoning, P.R. China

15 ⁶ Department of Microbiology, University of Tennessee, Knoxville, TN

16 ⁷ Department of Civil and Environmental Engineering, University of Tennessee, Knoxville, TN

17 ⁸ Department of Biology, Juniata College, Huntingdon, PA

18 ⁹ Earth & Planetary Sciences, University of Tennessee, Knoxville, TN

19 ¹⁰ Institute for a Secure and Sustainable Environment, Knoxville, TN.

20
21 *Corresponding Author, e-mail: tchazen@utk.edu. Phone: 865-974-7709. Address: 507 SERF,

22 University of Tennessee, Knoxville, TN 37996-1605

23

Abstract

Production of unconventional oil and gas continues to rise, but the effects of high-density hydraulic fracturing (HF) activity near aquatic ecosystems are not fully understood. A commonly used biocide in HF, 2,2-dibromo-3-nitrilopropionamide (DBNPA), was studied in microcosms of HF-impacted vs. HF-unimpacted surface water streams to (1) compare the microbial community response, (2) investigate DBNPA degradation products based on past HF exposure, and (3) compare the microbial community response differences and similarities between the HF biocides DBNPA and glutaraldehyde. The microbial community responded to DBNPA differently in HF-impacted vs. HF-unimpacted microcosms in terms of 16S rRNA gene copies quantified, alpha and beta diversity, and differential abundance analyses of microbial community composition through time. The difference in microbial community changes affected degradation dynamics. HF-impacted microbial communities were more sensitive to DBNPA, causing the biocide and byproducts of the degradation to persist for longer than in HF-unimpacted microcosms. Seventeen DBNPA byproducts were detected, many of them not widely known as DBNPA byproducts. Many of the believed to be uncharacterized brominated byproducts detected may pose environmental and health impacts. Similar taxa were able to tolerate glutaraldehyde and DBNPA, however DBNPA was not as effective for microbial control as indicated by a smaller overall decrease of 16S rRNA gene copies/mL after exposure to the biocide and a more diverse set of taxa was able to tolerate it. These findings suggest that past HF activity in streams can affect the microbial community response to environmental perturbation such as the biocide DBNPA.

Importance

Unconventional oil and gas activity can affect pH, total organic carbon, and microbial communities in surface water altering their ability to respond to new environmental and/or anthropogenic perturbations. These findings demonstrate that DBNPA, a common hydraulic

fracturing (HF) biocide, affects microbial communities differently as a consequence of past HF exposure, persisting longer in HF-impacted waters. These findings also demonstrate that DBNPA has low efficacy in environmental microbial communities regardless of HF impact. These findings are of interest, as understanding microbial responses is key for formulating remediation strategies in UOG impacted environments. Moreover, some of DBNPA degradation byproducts are even more toxic and recalcitrant than DBNPA itself, and this work identifies novel brominated degradation byproducts formed.

INTRODUCTION

Unconventional oil and gas (UOG) extraction has revolutionized the energy industry in the U.S. The use of hydraulic fracturing (HF) has made previously unreachable UOG reserves available for economically feasible extraction and pushed the U.S. towards energy independence (1). Multiple environmental concerns have accompanied this energy production growth. One of the most commonly added chemicals to HF fluids are biocides. Biocides are used in HF operations to control microbially-induced corrosion of casings and pipes, and gas souring caused by acid-producing and sulfate-reducing bacteria (2). However, biocides have warranted concern for several reasons. Biocides have varying degrees of reported efficacy due to potential resistance or inactivation of the biocides in HF conditions (2-5). Additionally, their toxicity and potential impact on the environment remains a contentious topic (2, 6). The fate of these biocides in the environment and their impact on microbial communities are poorly understood.

The biocide 2,2-dibromo-3-nitrilopropionamide (DBNPA) is the second most commonly used biocide in UOG after glutaraldehyde. DBNPA is a fast-acting electrophilic biocide, it is quick and effective in contact, but the protection is not long lasting (7). This biocide inhibits essential biological functions by reacting with nucleophiles (particularly sulfur-containing) inside the cell (8). DBNPA, and some of its degradation products, can also be harmful to humans and animals. These associated compounds have been demonstrated to be moderately to highly toxic

76 by ingestion and inhalation , can be corrosive to eyes, and can cause developmental issues in
77 terrestrial and aquatic animal studies (9, 10).

78 DBNPA is not toxic to all life, however, as it is biodegradable under both aerobic and
79 anaerobic conditions, with a reported biotic half-life of fewer than 4 hours for both at neutral pH
80 (10). However, the hydrolysis and aquatic photolysis half-life of this compound are pH-
81 dependent, with faster degradation occurring at a more alkaline pHs. For example, the abiotic
82 half-life of DBNPA at a pH 5, 7, and 9 is 67 days, 63 hours, and 73 minutes respectively (10).
83 Conversely, low pH has been characteristic of HF-impacted streams (11, 12), thus providing
84 favorable conditions for the stability of DBNPA and its degradation products.

85 The products of DBNPA biodegradation are the same under aerobic and anaerobic
86 metabolism (10). Still, the relative abundance of these degradation intermediates and their
87 reported half-lives varies depending on conditions such as pH, hydrolysis, photolysis, nucleophile
88 presence, and aerobic or anaerobic conditions (10, 13). There are two known degradation
89 pathways of DBNPA (Figure S1). The first pathway involves the hydrolysis of DBNPA into
90 dibromoacetonitrile (DBAN) \rightarrow dibromoacetamide (DBAM) \rightarrow dibromoacetic acid. DBAN is
91 more recalcitrant and three times more toxic than DBNPA (13). Dibromoacetic acid, a
92 problematic disinfection-by-product (14), has a half-life of 300 days and breaks into glyoxylic
93 acid, oxalic acid, bromide ions and carbon dioxide (15). However, a higher presence of total
94 organic carbon (TOC) and/or nucleophilic reactions under ultraviolet light favors a second
95 degradation pathway, where DBNPA degrades to monobromonitrilopropionamide (MBNPA), a
96 compound two times less toxic than DBNPA (13), and then to cyanoacetamide (CAM) (13, 15). It
97 was previously shown that HF-impacted streams have higher dissolved organic carbon than HF-
98 unimpacted streams (16), which may impact DBNPA degradation products in impacted
99 environments.

100 DBNPA can reach the environment in many ways; surface spills into the soil, surface
101 water, and aquifers; incomplete removal after water treatment; groundwater contamination after

equipment failure (leakage), and unintended fractures or abandoned wells (2). DBNPA environmental contamination could also occur in several of the steps associated with HF operations e.g., the transportation of chemicals to the site; mixing of HF fluids and chemicals on site; subsurface injection of the HF fluids; handling, collection, and storage of produce water; and disposal of the produced water (17). Understanding the impacts of surface and shallow groundwater spills, leaks, and disposal of poorly treated HF wastewater in the environment is of great concern as several studies have reported cases of the accumulation of toxic chemicals (such as hydrocarbons, benzene, toluene, ethylbenzene, and xylene, diesel, chlorinated solvents, among others) in groundwater, streams, soils, and sediments at HF operating sites (18-22). However, no study has investigated DBNPA degradation by-products and the microbial community changes over time in aerobic stream waters impacted by HF. This study aims to (1) understand the differences in local stream microbial community responses to DBNPA, (2) identification of DBNPA degradation by-products in streams impacted and unimpacted by HF operations, and (3) compare the microbial community response differences and similarities between the HF biocides DBNPA and glutaraldehyde.

RESULTS AND DISCUSSION

Quantification of bacterial 16S rRNA gene abundance over time

The 16S rRNA gene abundance was quantified at various points through the course of the experiment (Figure 1). Prior to DBNPA addition, the starting mean 16S rRNA gene concentrations were $4.03 \pm 0.60 \times 10^4$ gene copies/mL in the HF- impacted streams microcosms (HF+) and $4.38 \pm 0.50 \times 10^4$ gene copies/mL in HF-unimpacted streams microcosms (HF-). This difference was not statistically significant. Bacterial 16S rRNA gene in microcosms from two HF+ streams (Little Laurel, LL and Naval Hollow, NH) decrease immediately following addition of DBNPA and then increase, while Alex Branch (AB) displayed an increase in bacterial 16S rRNA gene concentration by day 7. In contrast 16S rRNA gene abundance in microcosms from two HF- streams (East Elk, EE and West Elk, WE) increase, while Dixon Run (DR) experienced

128 a decrease in 16S rRNA gene concentration by day 7. Specifically, seven days after addition of
129 DBNPA an average decrease of $-0.16 \log_2$ fold change (FC) in 16S rRNA gene copies/mL was
130 observed in HF+ microcosms, and a small average increase of $0.22 \log_2$ FC was observed in HF-
131 microcosms, indicating more sensitivity to DBNPA in HF+ microcosms. However, by day 56 the
132 HF+ experienced a $4.9 \log_2$ FC and HF- experienced a $3.9 \log_2$ FC. The difference in averaged
133 16S rRNA gene copies/mL through time (day 7 to 56) between HF+ and HF- microcosms was
134 statistically significant ($p < 0.05$). At day 56, the HF+ and HF- controls (no DBNPA added
135 microcosms) were not significantly different from each other, both experienced an $8.3 \log_2$ FC
136 from the initial gene copies/mL at day zero. The similitude in starting microbial abundance prior
137 to DBNPA addition indicates that the difference in microbial abundance observed after DBNPA
138 addition was due to the initial impact of DBNPA on the microbial community, followed by its
139 response and adaptation to the biocide, and low biocidal activity of DBNPA over time.

140 Quantification of the 16S rRNA gene shows that the HF- microbial communities were
141 initially more resistant and/or tolerant to the DBNPA perturbation, as shown by the overall
142 positive log-fold change in the gene copy number at day 7. DBNPA is a fast-kill biocide, thus
143 resistance at the initial time point is indicative of inefficacy of microbial control in HF-
144 microcosms. Through time, both HF- and HF+ showed strong resilience and adaptation to
145 decreasing concentration of DBNPA, however by day 56 HF+ had an overall greater gene
146 copies/mL (Figure 1) and the log-fold change than HF-.

147 There is no indication that the HF+ streams had any prior exposure to DBNPA prior to
148 this experiment. UOG operators in the area have disclosed the use of other biocides, such as
149 glutaraldehyde (reported in self-disclosing website fracfocus.org). Thus, prior exposure to HF
150 activity, not containing DBNPA, did not appear to provide 'priming' or a competitive advantage
151 to DBNPA exposure based on 16S rRNA gene copies/mL alone, but it provided favorable
152 conditions for quicker resilience (23). Furthermore, quantification of the 16S rRNA gene copy
153 number shows that there is overall environmental tolerance to high concentration of DBNPA,

154 indicating DBNPA is not as effective in controlling complex and dynamic microbial communities
155 as compared to environmental isolates or engineered systems (9, 24).

156 **Microbial Community Structural Changes**

157 Microorganisms in headwater ecosystems are environmental regulators of natural
158 geochemical cycles and organic matter cycling (25, 26). Microorganisms are very sensitive to
159 perturbation making them good sensors of environmental change and effective for tracking
160 contaminants (27). Before DBNPA addition HF- microcosms had an overall higher evenness and
161 richness than HF+. After addition of DBNPA, evenness and richness were affected through time
162 in both HF+ and HF- microcosms. Shannon diversity, which account for the abundance and
163 evenness of species present, showed that HF+ microcosms experienced a smaller decrease in
164 evenness and richness—even though HF- had an overall higher diversity (Figure 2a) ($P < 0.01$).
165 Meanwhile, while not statistically significant, Simpson diversity (Figure 2d) which also accounts
166 for the abundance of species present, indicated minimal changes in diversity over time except for
167 HF- at day 21. Still, diversity increased by day 35. In contrast, Chao1 ($P < 0.05$) and Observed (P
168 < 0.05) measurements (Figure 2b and 2c), which include unique and rare operational taxonomic
169 units (OTUs) in their calculations, experienced a more prominent decrease in diversity, as fewer
170 OTUs dominated over time. In contrast, when comparing day zero with day 56 control to test
171 bottle effect, the changes detected by day were not significant, and HF- maintained higher
172 diversity than HF+.

173 Analysis of weighted UniFrac distances between samples revealed that there was a
174 difference in phylogenetic composition response between HF+ and HF- microbial populations.
175 The weighted UniFrac distances were plotted on a directional Principal Coordinate Analysis
176 (PCoA), PC 1, explained 27.90 % of the sample variance, while PC2, explained 17.99% of the
177 sample variance (Figure 3). At day zero, prior to DBNPA addition HF+ and HF- already clustered
178 separately along the PC1 axis, but after DBNPA addition HF+ and HF- visibly separated more
179 over time, showing that the HF+ and HF- got more dissimilar over time after addition of DBNPA.

180 Meanwhile the HF+ and HF- no-DBNPA added controls cluster together at day 56. Permutational
181 multivariate analysis of variance (PERMANOVA) indicated that there were statistically
182 significant differences between HF+ and HF- microbial community through time (Table 1). This
183 difference indicates that DBNPA selected for different sets of taxa based on HF exposure.

184 **Differentially Enriched Taxa Over Time and Between HF+ and HF- Microcosms**

185 The initial bacterial population (before DBNPA amendment) in all microcosms,
186 regardless of HF history, was predominantly *Proteobacteria*, which comprised more than 75.5%
187 $\pm 4.8\%$ of 16S rRNA gene reads in HF+ and more than $64.4\% \pm 3.2\%$ in the HF- group.
188 *Proteobacteria* were expected to dominate, as previous studies on these Pennsylvania streams
189 reported this phylum as the principal population (11, 12, 16). However, initial proportions of
190 *Beta*, *Alpha*, and *Gammaproteobacteria*, in that order of abundance differed between the HF+
191 and HF- groups. Taxa plots illustrate the difference in microbial community structure over time
192 (Figure S2a and S2b). *Gammaproteobacteria* were the first responders in both HF and HF- after 7
193 days of DBNPA addition with *Pseudoalteromonadaceae* as the most dominant family at this
194 time, $12.3\% \pm 4.0\%$ of HF+ microcosms and $19.4\% \pm 2.2\%$ of HF- microcosms. A strong
195 correlation between *Gammaproteobacteria* and HF+ streams has been shown before (11, 12). By
196 day 35, *Alphaproteobacteria*, specifically, the genus *Methylobacterium* was the most dominant
197 taxa ($15.6\% \pm 7.7\%$ in HF+ and $30.5\% \pm 6.2\%$ in HF-). However, by day 56 a more diverse
198 microbial composition was observed, with few overall dominant taxa. In HF+ the most dominant
199 taxa were Unclassified bacteria ($10\% \pm 5.1\%$), *Comamonadaceae* ($9.5\% \pm 2.7\%$),
200 *Alcanivoracaceae* ($8.9\% \pm 7.8\%$), and *Sphingomonadaceae* ($7.9\% \pm 2.4\%$), and in HF- the most
201 dominant taxa were *Comamonadaceae* ($6.3\% \pm 0.8\%$), auto67_4w from the order
202 *Pedospaerales* ($5.7\% \pm 1.3\%$), and *Methylobacteriaceae* ($6.3\% \pm 2.7\%$) (Figure 4).

203 There were important changes to the microbial community structure in both HF+ and HF-
204 following amendment with DBNPA. Seven days after DBNPA amendment, the relative
205 abundance of 29 taxa were significantly different (DESeq2, Wald Test $P \Rightarrow 0.01$) in both HF+

206 and HF- compared to day zero; 24 of which increased in relative abundance, and five decreased
207 (Table S1). The two taxa with the highest increase were identified as the family AEGEAN 185
208 (7.43 log₂FC) from the SAR404 phylum, and family SAR 324 (7.26 log₂FC) a member of the
209 class *Deltaproteobacteria*. Both of these taxa were reported in a similar experiment using the
210 biocide glutaraldehyde (28). AEGEAN 185 matches to sequences of a clone library from the
211 North Aegean Sea, but its metabolic profile is unknown (29). Sequenced members of SAR 324
212 are known to possess genes for methane monooxygenase and dehalogenases that, if expressed,
213 can co-metabolize halogenated compounds such as DBNPA (30-32). The only enriched genus
214 with a relative abundance greater than 2% at all time points in the experiment was *Alcanivorax*
215 (3.27 log₂FC). *Alcanivorax* is a known oil degrader (33) and was also enriched in glutaraldehyde
216 microcosms, showing a wide range of xenobiotic compounds it is capable of tolerating, and even
217 possibly degrading (28). In addition to the three previously mentioned taxa, 9 more were enriched
218 with both glutaraldehyde and DBNPA: *Achromobacter*, *Synechococcus*, SarSea-WGS and
219 Artic95A-2 from the SAR 406 clade, *Acidimicrobiales*, *Nitrospina*, *Sphingopyxis* and
220 *Euryarchaeota* Marine group II and III. Of the five suppressed OTUs, three were from the order
221 *Burkholderiales*. Differential abundance analysis between HF+ and HF- at day 7 showed 51 taxa
222 were significantly different; 30 were enriched in HF+, and 21 were enriched in HF- (Table S2).
223 The most substantial log FC was *Micrococcus* (6.14 log₂FC), and the taxa that were enriched and
224 comprised more than 2% relative abundance in HF+ were *Verrucomicrobiaceae*,
225 *Caulobacteraceae*, *Janthinobacterium*, *Novosphingobium*, *Oxalobacteraceae*, and
226 *Limnohabitans*.
227 The microbial communities at days 21, 35, 49, and 56 (Tables S3, S4, S5, and S6,
228 respectively) followed a similar trend, with approximately 100 differentially enriched taxa in both
229 HF+ and HF- microcosms compared to day zero. Through time, many OTUs related to marine
230 environments such as *Idiomarina*, SAR 324, Aegean-185, *Alteromonadaceae*, ZD017, *Halomonas*,
231 and *Alcanivorax* were enriched. Enrichment of marine taxa is notable as osmotic regulation and

232 efflux pumps, which are important attributes of marine microbes, have been linked to biocide
233 tolerance (34-37) but mechanistic details about microbial tolerance to DBNPA have not been
234 previously reported. Marine organisms are found in low abundance in freshwater streams, and
235 they can bloom when conditions are favorable (38), which indicates a potential competitive
236 advantage of halotolerant bacteria to DBNPA. For example, a halotolerant *Halomonadaceae* was
237 shown to be enriched in HF exposed anaerobic sediments treated with DBNPA (39). Other
238 halotolerant bacteria have also emerged as bacterial biomarkers of UOG impacts in freshwater
239 streams (40). HF fluids contain high abundance of halophilic and halotolerant bacteria (41),
240 which can be displaced to streams in the event of an HF fluid spill.

241 Other differently enriched organisms between days 21, 35, 49, and 56 (Tables S3, S4, S5,
242 and S6, respectively) included *Dietzia*, *Bacillus*, *Methylobacterium*, *Verrucomicrobiaceae*,
243 *Novosphingobium*, *Caulobacteraceae*, among others. *Dietzia* was previously shown to resist
244 antimicrobials in freshwater and wastewater ecosystems (42). *Bacillus* has been reported to
245 possess intrinsic resistance to antimicrobial as they can form spores when antimicrobial pressure
246 is encounter (43, 44). Bacterial spores are the least susceptible to biocidal action (43).
247 *Methylobacterium* is a common environmental microbe that was previously shown to be enriched
248 and dominant after freshwater consortium was exposed to glutaraldehyde (28), and species in this
249 genus have been shown to be resistant to other antimicrobials (45). Another microcosms study
250 using sediment and water anaerobic mixture showed that DBNPA exposure decreased
251 *Methylobacteriaceae* abundance (39), indicating that oxygen availability is needed for
252 *Methylobacterium* resistance and enrichment in the presence of DBNPA. *Novosphingobium* are
253 commonly found in environments impacted by anthropogenic activity (46). They are known to be
254 effective biodegraders of toxic and recalcitrant compounds (46). However, the family
255 *Sphingomonadaceae*, which *Novosphingobium* is a member of, also was shown to decrease after
256 exposure to DBNPA in a previous anaerobic sediment and water microcosms (39), indicating
257 again that oxygen or sediment presence affect tolerance and resistance of this taxa. Taxa enriched

258 in HF+ but not HF- included *Verrumicrobiaceae* and *Caulobacteraceae* which were shown by
259 another study to be susceptible to a low dosage of DBNPA in sediments that were not exposed to
260 HF (39). The enrichment of these taxa only in HF+ microcosms may indicate that prior exposure
261 to HF fluids can build tolerance to DBNPA in *Verrimicrobiaceae* and *Caulobacteraceae*
262 regardless if HF fluids contained DBNPA. Furthermore, *Caulobacteraceae* has been previously
263 identified as a microbial biomarker of UOG activity in streams in PA (40).

264 At day 56, the negative control had 209 differentially enriched taxa compared to day
265 zero, which can be attributed to bottle effect (Table S11). Meanwhile, at day 56 the experimental
266 and negative control microcosms (no DBNPA added) had 181 differentially enriched taxa. Of
267 those, 111 were enriched in the experimental microcosms (Table S12), which, when summarized
268 at genus level, reveals that *Bacillus*, *Idiomarina*, *Glaciecola*, *Alcanivorax*, *Acinetobacter*, *Vibrio*,
269 *Dietzia*, *Methylobacterium*, *Pseudoalteromonas*, *Marinobacter*, *Novosphingobium*,
270 *Stenotrophomonas*, *Burkholderia*, and *Oxalobacteraceae* (unclassified genus) show tolerance and
271 adaptation to DBNPA.

272 Another study used .0025% v/v DBNPA with and without the addition of FeOOH in
273 anaerobic microcosms constructed with sediment inoculum from up- and downstream from a
274 UOG wastewater treatment facility to understand how UOG wastewater processing affects
275 downstream microbial communities and how those changes affect anaerobic microbial responses
276 to HF fluid additives (39). That study found three enriched families in the UOG-downstream
277 microcosms amended with only DBNPA and two of those, *Halomonadaceae* and
278 *Staphylococcaceae*, were also found in this study. Conversely, the same UOG downstream
279 samples were amended with FeOOH and DBNPA, and six families were enriched, two of which
280 were also detected in this study: *Rhodospirillaceae* (enriched over time in HF+ as compared to
281 HF-, Tables S2, S7 to S10), and *Ignavibacteriaceae* (enriched at days 21 and 35, Table S3 and
282 S4). However, the study by Mumford et al. (2018) only sample at day 42 after incubation, and the

low DBNPA concentration, sediment, and anaerobic conditions used are expected to result in wide differences between that study and the one described here.

Microbial community responses to DBNPA vs. Glutaraldehyde

We recently conducted a similar study using 100 mg/L of the biocide glutaraldehyde (28). The changes in microbial abundance observed after treatment with DBNPA contrast with the results of the glutaraldehyde experiment. In the glutaraldehyde study, all of the six stream microcosms experienced an initial decrease in microbial abundance. On average HF+ communities were initially more resistant to the biocide, as observed by a smaller log-fold change of 16S rRNA gene/mL by day 7. By day 56, HF- showed stronger resilience by having a bigger positive log-fold change. These results show that the microbial abundance adaptation response in these microbial communities is biocide specific.

Methylobacterium, *Idiomarina*, *Bacillus*, and *Alcanivorax*, among others, were enriched in the presence of both DBNPA and glutaraldehyde (28). The enrichments indicate that these taxa have a competitive advantage when exposed to these two electrophilic biocides. Previous studies have shown that glutaraldehyde resistance may be caused by the expression of efflux pumps (36, 47). However, the mechanisms for DBNPA resistance is not known, and functional genomics and transcriptomics analyses are needed to better understand this mechanism.

Furthermore, Weighted UniFrac beta diversity (Figure 3) showed a distinct phylogenetic response between HF+ and HF- microcosms. This was similar to what was observed in previous work (28), yet glutaraldehyde showed more significant phylogenetic distances on a PCoA plot. The primary axis explained 65.4 % of the variation and the second axis explained 10%, while for DBNPA PC1 and PC2 explained 27.90% and 17.99% respectively, showing that the response and phylogenetic changes due to DBNPA addition were not as pronounced as for glutaraldehyde. Even though both are electrophilic biocides, DBNPA is a fast kill biocide while glutaraldehyde biocidal properties are longer lasting (2). Glutaraldehyde is also more persistent over time (28), with a biotic half-life of 33.8 d in HF- and a biotic half-life of 51.9 in HF+, potentially explaining

the more pronounced differences in the phylogenetic distribution of glutaraldehyde-treated microcosms over time. Furthermore, the alpha diversity changes and the differentially enriched taxa suggested that the microcosms contain a higher quantity of OTUs that are able to tolerate and adapt to DBNPA as compared to having just a few OTUs becoming enriched as in the case of glutaraldehyde (28). For example, *Methylobacterium* was the most dominant taxa by day 35 in the microcosms exposed to DBNPA (15.6% in HF+ and 30.5% in HF-) , but by day 56 there is not clear dominating taxa. In contrast, when exposed to glutaraldehyde *Methylobacterium* dominated the community from day 21 throughout day 56. At this final time point *Methylobacterium* represented 70.6% of the observed microbial community HF+ and 84.2% in HF- (28). Based on this comparison, combined with the significant increase in 16S rRNA gene copies, it seems that DBNPA tolerance is more ubiquitous. There are multiple possible explanations for this result: (1) changes in the microbial community structure and/or adaptation of individual community members improves resilience of the community as a whole, and (2) DBNPA is degraded either biotically or abiotically more rapidly than glutaraldehyde (28, 48, 49).

Abiotic and Biotic Transformation of DBNPA

We evaluated the degradation of DBNPA over 56 days (d) using both biotic and abiotic microcosms constructed from HF+ and HF- streams (Figure S3 and Figure S4). However, the degradation rate of DBNPA could not be calculated as quantification by HPLC-DAD revealed a sharp increase in DBNPA signal at day 14 at two of the HF+ sites with documented spills (AB and LL, both biotic and abiotic samples). The sharp increase in DBNPA signal could not be attributed to human error, or equipment malfunction (Figure S3 and Figure S4). It is possible that a coeluting compound was absorbed in the same region or interfered with the HPLC-DAD measurement, which could explain the spike at day 14 (Figure S4), due to chromophores and/or similar degradation products that may not be distinguishable with this method (50) . However, DBNPA non-detection was achieved by all HF- biotic microcosms sets (28 d for EE, 49 d for WE, and 56 d for DR), while only one HF+ biotic microcosm set reached non-detection (56 d for

335 NH). Conversely, only one HF- abiotic microcosms set reached DBNPA non-detection (49 d for
336 EE) and only one HF+ abiotic microcosm set (56 d for NH). These observations indicate HF-
337 microbial communities were better at tolerating and degrading DBNPA.

338 DBNPA degradation has been documented previously (10, 13, 15). It was shown by
339 others that degradation rate of this biocide is pH dependent with degradation rates inversely
340 proportional to pH (10, 15). In this study, HF+ streams had an average pH of 4.9 ± 0.13 and HF-
341 streams had a pH of 6.5 ± 0.46 (Table S15), and HF- microcosms depleted DBNPA faster than
342 HF+ which agrees with the pH dependent degradation trends previously reported (10, 15). The
343 only biotic HF+ microcosm set to reach non-detect was NH which had the least acidic pH of the
344 set (Table S15). However pH based hydrolysis was not the only factor contributing to degradation
345 as abiotic microcosms were not able to reach non-detect at the same speed, indicating microbial
346 biodegradation also played a role.

347 To evaluate whether a contaminant or degradation product with similar absorbance and
348 retention time as DBNPA may be contributing to the DBNPA signal, the biotic and abiotic
349 samples from days 0, 7, 14, 21, and 28 from the HF+ sites (AB and LL) and also two HF- sites
350 for comparison (WE and EE) were analyzed using nano-HPLC-HRMS. High mass accuracy
351 measurements (± 5 ppm) and fragmentation data from the LC-MS were used to qualitatively
352 evaluate the results, first by searching for DBNPA and known degradation products, and then by
353 comparing the number of brominated compounds detected. Then, relative abundance values and
354 integrated peak area were used to evaluate the trends of these compounds across the five time
355 points within each sample set. The DBNPA molecular ion ($[M+H]^+ = 240.8606$ m/z) was not
356 detected in most of the samples analyzed, which may be due to prolonged storage or multiple
357 freeze-thaw cycles (each sample experienced 2 freeze-thaw cycles). However, because bromine
358 (Br) has a unique isotopic signature (Figure S5), multiple other brominated species were
359 observed; some of which were known DBNPA degradation products, but many were previously-
360 unreported species and potentially novel brominated degradation products (Table S13). Across

the four sites (WE, EE, AB, LL), five time points (day zero to 28), and two microcosm conditions (biotic or abiotic) analyzed ($n = 40$), 18 brominated species were observed, including DBNPA and four known degradation products: CAM, MBNPA, DBAN, and DBAM (Figure S1, Table S13). The detected mass to charge ratio, predicted elemental formula, and putative structure of some of these brominated products are described in Table S13. More brominated species were detected in the abiotic samples (an average of 14.1 ± 2.8) compared to the biotic samples (11.7 ± 4.4) (Figure S6). There were also more brominated species in the biotic HF- samples (13 ± 5.6) than the biotic HF+ samples (10.4 ± 3.3) and in abiotic HF- samples (15.2 ± 3.5) than the abiotic HF+ samples (13 ± 1.7) (Figure S6). Number of brominated compounds increased through time in all samples (Figure 4), indicating the formation of byproducts of degradation or reaction of bromide with available organics in the water. Similar to the trend observed by HPLC-DAD, the number of brominated species detected by LC-MS in the HF+ abiotic samples (AB and LL) increased sharply from day zero to day 14 (Figure S6). The total “brominated signal” (summed, integrated peak areas at each time point) also increased sharply at day 14 in the abiotic HF+ samples (Figure S7). While not as strong, the brominated signal also increased at day 14 in the two abiotic HF- samples. For the biotic samples, a steady increase in brominated signal over time was observed regardless of the microcosm, with the highest signal occurring at day 21. The qualitative trends are consistent with the initial HPLC-DAD measurement, which suggests that these brominated degradation products may indeed have impacted the signal response in the initial measurement.

MBNPA and CAM, two known degradation products of the less toxic degradation pathway (Figure S1), were detected in abiotic and biotic in both HF+ microcosms (AB and LL) and one HF- (EE). DBAN, toxic pathway degradation product (Figure S1) was detected in the biotic LL microcosms (HF+) and abiotic and biotic EE microcosms (HF-), while DBAM, another toxic degradation pathway product, was detected in both biotic AB and LL (HF+) and only abiotic LL, while both abiotic and biotic WE and EE (HF-). Others have shown that the

387 preference for one degradation pathway is dependent on total organic carbon (TOC) content, and
388 that higher TOC selects for the less toxic pathway, with MBNPA as an intermediate (13). It is
389 documented that HF+ streams in PA, including AB and LL, have higher dissolved organic carbon
390 than HF- due to land clearing practices from well-pad development (16). Here, mean TOC (Table
391 S14) at day zero was significantly higher in HF+ samples (7.81 ± 1.11 mg/L) than in HF- samples
392 (4.09 ± 0.95 mg/L; *t*-test, *P* = 0.02), which could explain the presence of the nontoxic pathway
393 intermediates at the HF+ microcosms, TOC could also be reacting with bromine left after
394 complete DBNPA degradation. Other factors to consider include different enzymatic capabilities
395 of the microbial communities present within the samples or different water chemistries favoring
396 one pathway over another. The water chemistry measured *in situ* (Table S15) was reported
397 previously: temperature (HF+: $16.8^{\circ}\text{C} \pm 1.96$, HF-: $12.8^{\circ}\text{C} \pm 0.58$), pH (HF+: 4.9 ± 0.13 , HF-:
398 6.5 ± 0.46), conductivity (HF+: 29.2 ± 3.67 $\mu\text{S}/\text{cm}$, HF-: 33.7 ± 5.66 $\mu\text{S}/\text{cm}$), and total dissolved
399 solids (HF+: 20.8 ± 2.80 mg/L, HF-: 23.9 ± 4.01 mg/L) (28). Even though the differences in these
400 parameters were not significantly different between HF+ and HF-, the differences in pH may
401 affect the stability of DBNPA as discussed previously. This observation is also supported by
402 cluster analysis as the detected brominated species clustered by HF impact history (Figure 5a).
403 Samples also clustered by biotic and abiotic conditions per stream, indicating that microbial
404 presence affected the degradation byproducts (Figure 5b). Overall, these results suggest that
405 DBAM and other brominated species may be persistent degradation products of DBNPA that,
406 depending on the history of the watershed, may be preferentially selected over the desired less
407 toxic pathway with MBAN and CAM as intermediates. More DBNPA degradation kinetic
408 experiments are needed to better understand the conditions dictating intermediate formation.

409 **Environmental Implications**

410 Our findings demonstrate that previous HF exposure causes surface water microbial
411 communities to respond differently to the biocide DBNPA as compared to HF-unimpacted

412 communities. HF exposure history, and its effect in water chemistry and microbial interactions,
413 may also affect the formation of DBNPA brominated degradation products. In a similar
414 experiment using glutaraldehyde, a distinct microbial community was enriched between HF+ and
415 HF- after glutaraldehyde perturbation. In the glutaraldehyde experiment the HF+ microbial
416 community showed higher tolerance to glutaraldehyde based on higher diversity and a smaller log
417 fold decrease of the 16S rRNA gene concentration, but HF- microbial community was able to
418 degrade glutaraldehyde faster. The faster glutaraldehyde biodegradation in HF- was attributed to
419 biotic-abiotic interactions as HF+ had acidic pH compared to HF- (28), as glutaraldehyde activity
420 is enhanced at alkaline pH (51). Alkaline pH forms more reactive sites in the cell wall, this effect
421 allows more bacteria to be susceptible to glutaraldehyde while depleting the glutaraldehyde in
422 solution as it cross-links with the bacterial wall (51).

423 DBNPA caused a different microbial response than the biocide glutaraldehyde. First, HF-
424 microcosms were better at tolerating DBNPA based on initial 16S rRNA log fold change, which
425 is opposite to what was observed with glutaraldehyde. This could be in part due to DBNPA faster
426 hydrolysis at increasing pH, causing HF- microcosms to deplete DBNPA faster as compare to the
427 more acidic HF+ microcosms. Second, even though similar microbial groups were enriched, a
428 more diverse microbial population was able to resist DBNPA as compared to glutaraldehyde, as
429 *Methylobacterium* enrichment represented up to 92% of glutaraldehyde microcosms (28). The
430 difference in microbial response may be caused by the DBNPA fast-kill approach, where its
431 biocidal activity is more potent at the moment of initial contact, while glutaraldehyde works over
432 a period of days to weeks. However, both DBNPA and glutaraldehyde depletion was faster in
433 HF- microcosms.

434 This study revealed that DBNPA and associated degradation products can be persistent in
435 stream water. TOC could have a role in the formation of degradation products. These findings are
436 of importance, as environmental persistence may further hinder the return of the microbial
437 communities to pre-impacted states affecting nutrient cycle, and further retard microbial natural

438 biodegradation capabilities (i.e. microbial attenuation) in the environment, potentially requiring
439 intervention to stimulate the affected area to enhance the preference for DBNPA non-toxic
440 degradation pathways. Environmental persistence of the brominated disinfectant by-products can
441 cause harm to the public and environmental health. For example, the persistence of these
442 disinfectant by-products may affect ecosystem function, e.g. microbial primary production and
443 natural attenuation which could have unknown cascading effects to higher trophic levels (10, 52-
444 55). Broad HF impacts have already been shown to affect micro and macroinvertebrates, fish and
445 other aquatic organisms in the streams used as source water for the microcosms (16, 56).

446 Many of the taxa enriched in this study have been previously reported as being capable of
447 degrading or co-metabolizing xenobiotic compounds. Although a genetic pathways for microbial
448 biodegradation of DBNPA has not been determined, as a halogenated compound, it is likely that
449 the aerobic degradation pathways would involve cometabolism, aerobic assimilation, or
450 dehalogenation (57, 58). In the non-toxic degradation pathway of DBNPA (Figure S1), the
451 bromines are substituted by hydrogen, which could be achieved by microbial reductive
452 dehalogenation (59), and by abiotic mechanisms. For example, AB and LL (HF+ streams)
453 derived microcosms showed intermediates of the less toxic degradation pathway, in both biotic
454 and abiotic conditions, but MBNPA was an order of magnitude higher in biotic conditions
455 (Figure 5b), leading to the conclusion that microbial biodegradation is active and rapid compared
456 to abiotic degradation alone. Further research is needed to understand which microbes can use
457 DBNPA as a carbon source, electron donor, or electron acceptor in metabolism.

458 Additional research is needed to determine a complete degradation pathway, including
459 quantification of all brominated intermediates, and to better understand when one DBNPA
460 degradation pathway is preferred over the other to adequately handle a HF chemical spill
461 containing DBNPA. Furthermore, differences in degradation kinetics of DBNPA and associate
462 degradation products between HF+ watersheds and pristine should be determined to quantify and
463 determine under what conditions HF+ microbial communities are more efficient at debrominating

464 DBNPA and its degradation byproducts. DBNPA may not persist in the environment, but its
465 brominated degradation products, such as DBAN, have a longer half-life and could be more
466 harmful to the public and environmental health.

467

468 **MATERIALS AND METHODS**

469 **Stream Selection and Sample Collection**

470 For comparison purposes, sample collection was identical and done at the same time as
471 Campa et al., 2018 . Briefly, sample selection employed GIS surveys, and the Pennsylvania
472 Department of Environmental Protection (PADEP) records to minimize watershed variation
473 caused by industrial activities other than UOG extraction. Streams selected were in forested areas,
474 with no indication of past mining activity or other anthropogenic impacts in the PADEP records.
475 HF-impacted (HF+) streams had active UOG wells within the watershed. These streams were
476 Alex Branch (AB), Little Laurel (LL), and an unnamed tributary to Naval Hollow (NH). AB and
477 LL had reported surface spills (60-62). The spills occurred in 2009 when a pipe carrying
478 flowback water burst, leaking into LL, and to a lesser extent to AB. In the same year, HF
479 chemicals were accidentally spilled into AB. The three HF un-impacted (HF-) streams had
480 construction development involving well pads, but no HF activity had started. These streams
481 were UNT East Elk (EE), unnamed tributary to West Elk (WE), and Dixon Run (DR). Refer to
482 Table S15 for geological coordinates of the watersheds. A detailed description of the sites,
483 screening process and selection has been described previously (11-13, 56, 63).

484 Collection of stream water from three HF+ and three HF- streams in northwestern
485 Pennsylvania occurred in June 2015 under low flow conditions. Samples were collected in sterile
486 Nalgene bottles and stored at 4°C until use. Conductivity, pH, temperature, and total dissolved
487 solids were measured at collection time using a weekly calibrated Eutech PCSTestr 35 Multi-
488 parameter test probe.

489 **Microcosm Setup**

490 Dow Chemicals' literature showed effective kill (> 6 log reduction) of acid producing
491 bacteria (APB) and sulfate-reducing bacteria (SRB) using 25 mg/L of DBNPA (24); nevertheless,
492 biocide usage in HF is highly variable with reports between 10 to 800 mg/L (6). Thus,
493 microcosms were constructed using 125 mg/L DBNPA in 235 mL of stream water. DBNPA was
494 purchased from Sigma-Aldrich (CAS 10222-01-2). Abiotic controls were autoclaved to kill all
495 microbes present and were used to measure abiotic degradation of DBNPA. Negative biological
496 controls (No-DBNPA added) were used to examine the bottle effect in microbial communities
497 with no biocide added. Abiotic and biological controls were set at a volume of 20 mL. All
498 microcosms were set in triplicates at ambient temperature ($\sim 21^{\circ}\text{C}$) under aerobic conditions and
499 minimal light exposure for 56 days. Microcosms were uncovered only for sampling events and
500 were shaken before sampling. Samples were collected every seven days for chemical analysis and
501 day zero, 7, 21, 35, 49, and 56 for microbial analyses. TOC was measured before the beginning of
502 the experiment using a Shimadzu TOC-L Series analyzer with ASI-L autosampler (Shimadzu,
503 Kyoto, Japan) following the protocol described in Campa et al., 2018.

504 **Quantification of Bacterial 16S rRNA Gene**

505 DNA was collected by filtering 25 mL of microcosm water through a 0.2 μm nylon filter
506 (Sterivex), and frozen at -20°C until use. The frozen filter was cut with sterile pliers. The filter
507 membrane was cut with a sterile razor and DNA was extracted from the membrane using Mo Bio
508 PowerSoil DNA isolation kit following manufacturers specifications. Bacterial primers
509 Bac1055YF and Bac1392R were used to quantify the 16S rRNA gene in a QuantStudio 12K Flex
510 Real-Time PCR system (ThermoFisher Scientific). For reaction mixture, and qPCR parameters
511 refer to Campa et al. (2018).

512 **16S rRNA Gene Amplicon Library Preparation, Sequencing, and Data Analyses**

513 After DNA extraction, the v4 region of the 16S rRNA gene was amplified using the
514 primers and protocol described previously (64). Refer to Campa et al. (2018), for the description

515 of library preparation. The final libraries were run in the Illumina MiSeq (San Diego, CA, USA)
516 using a v2 (2 x 150 reads) kit following manufacturer's specifications.

517 Data analyses were done in QIIME (version 1.9.1) following the protocol described in
518 Campa et al. (2018). Briefly, after joining forward and reverse reads and demultiplexing, quality
519 filtration was set to an average Q-score of more than 19. De novo and reference-based chimera
520 detection was done using UCHIME in the USEARCH package (65, 66). OTU picking was done
521 using the Greengenes database (version May 2013)(67) applying a 97% sequence identity cut-off
522 using UCLUST(65). Representative sequences for each OTU were aligned using the PyNAST
523 method (68) and taxonomy was assigned using the RDP classifier (69). The OTU table was
524 filtered further to remove sequences with counts below 0.005% and any samples with less than
525 1000 sequences were discarded and the OTU table was cumulative-sum scaling (CSS) normalized
526 (70) for beta diversity, weighted UniFrac distance matrix calculation (71). Weighted Unifrac
527 distance matrix was visualized using a directional Principal Coordinate Analysis (PCoA) in
528 EMPeror (72) forcing the x-axis by days. The OTU table and weighted Unifrac was then
529 imported into R and the packages Phyloseq (73) and Vegan (74) were used for statistical analyses
530 as described below. An unnormalized OTU table was also exported into R for alpha diversity and
531 DESeq2 analyses (75, 76). Difference in alpha diversity metrics, Chao 1, Simpson, Shannon,
532 and Observed species, were computed using the package Phyloseq (73) to understand the
533 difference in evenness and richness between HF-impacted and HF-unimpacted microcosms
534 before and after DBNPA addition. Statistical analyses were performed as described in the next
535 section.

536 DESeq2 (76) R package was used to identify differentially enriched taxa through time
537 and between HF+ and HF- microcosms at each time point (day 7, 21, 35, 29, and 56) to day zero
538 no-DBNPA added controls. Day 56 DBNPA added microcosms and day 56 no-DBNPA added
539 controls were compared as well. Per time point, comparisons between HF impact status were also
540 made. For each comparison a Wald test was performed using the parametric fit-type and the P-

541 value was adjusted using Benjamini & Hochberg method. Reported OTUs had an $\alpha < 0.01$
542 and a reported $2 \log_2$ fold change or higher. following the protocol in Campa et al (2018). using a
543 cutoff of $2 \log_2$ fold change or higher, and a Bonferroni adjusted p-value of 0.01.

544 **Statistics**

545 For comparison purposes, statistical analysis was similar to that in Campa et al. (2018).
546 To understand the effect of DBNPA on microbial community, 16S rRNA gene abundance was
547 compared using a complete randomized design (CRD) with split plot using impact status (HF+
548 vs. HF-) as the whole plot factor and time (days) as the split-plot factors using a mixed effect
549 ANOVA model in the R nlme package (77). The least squares means were computed and
550 separated with the Bonferroni method using the R emmeans package (78). 16S rRNA gene
551 copies/mL were \log_{10} transformed to meet normality and variance assumptions for ANOVA. To
552 compare the no-biocide control at day zero and at the end of the experiment (day 56), the same
553 model was used. To determine the differences between HF+ and HF- at day zero, an independent
554 sample t-test was performed with data for only that time point. Microbial community alpha
555 diversity (Chao 1, Simpson, Shannon, and Observed species) values were rank transformed and
556 compared using the same model as for 16S rRNA gene copies/mL. Finally, microbial community
557 beta diversity weighted UniFrac distance matrix was used to compare temporal differences
558 between HF+ and HF- microcosms before and after DBNPA addition were applying a nested
559 PERMANOVA with 999 permutations using the adonis command in the Vegan (74) R package.
560 All statistical tests were performed using R, and p-value significance was set at $p = 0.05$. See
561 supplemental methods for R-scripts used.

562 **Quantification of DBNPA using HPLC-DAD**

563 Every week, 1 mL of microcosm water was collected to compare the difference between
564 the rates of abiotic and biotic DBNPA degradation in HF+ and HF- microcosms. After collection,
565 samples were filter-sterilized using $0.2 \mu\text{m}$ nylon filter, acidified to pH 2.5 with phosphoric acid

566 to minimize hydrolysis of DBNPA as described by Blanchard *et al.* (1987), and were then frozen
567 at -20°C until analysis.

568 DBNPA quantification was performed with an Agilent 1200 HPLC system using a
569 modified method described by Blanchard *et al.* (1987). An Agilent Eclipse XDB-C18 column (5
570 μm , 4.6 x 150 mm) was used for separation with a flowrate of 1 mL/min and a diode array
571 detector (DAD) was set at 210 nm for detection. The mobile phases and elution gradient were as
572 follows: The initial composition was 75% deionized water (adjusted to pH 2.5 with phosphoric
573 acid; eluent A) and 25% acetonitrile (eluent B), and eluent B increased linearly to 60% over 6
574 min and further to 85% over an additional 4 min time period. Eluent B was held at 85% for 1 min
575 before the column was equilibrated to initial conditions.

576 **Detection of DBNPA Degradation Products Using Nano-High Performance Liquid**

577 **Chromatography-High-Resolution Mass Spectrometry**

578 Filtered stream water samples were kept frozen in amber bottles in the dark at -20°C until
579 analysis by nano-liquid chromatography-high-resolution mass spectrometry (nano-HPLC-
580 HRMS). Measurements were collected using a Dionex UltiMate 3000 HPLC pump
581 (ThermoFisher Scientific) coupled to an LTQ-Orbitrap Velos Pro mass spectrometer
582 (ThermoFisher Scientific) equipped with a nano-electrospray ionization (ESI) source (Proxeon,
583 Denmark) operated in positive mode under direct control of the XCalibur software, v2.2 SP1.48
584 (ThermoFisher Scientific). The nano-electrospray column/emitter was prepared manually in-
585 house using 100 μm i.d. fused-silica (Polymicro Technologies) which was laser-pulled and
586 pressure-packed to 20 cm with Kinetex C18-RP material (5 μm , 100 Å, Phenomenex). The
587 column was aligned in front of the MS capillary inlet, and 300 nL of the sample was manually
588 injected directly onto the column. LC/MS-grade acetonitrile (ACN) and water (both degassed)
589 were purchased from EMD Millipore, and formic acid (FA) from Sigma-Aldrich. Nano-flow rates
590 were achieved with a split-flow setup prior to the injection loop ($\sim 250 \text{ nL min}^{-1}$ at the nano-spray
591 tip) and separations were conducted by initially holding at 100% A (95% ACN/5% H_2O /0.1%

592 FA) for 5 min, increasing linearly over 60 min to 100% B (70% ACN/30% H₂O/0.1% FA), and
593 then holding at 100% B for 5 min before re-equilibrating the column at 100% A for 20 min prior
594 the next injection.

595 The mass spectrometer was externally calibrated for mass accuracy on the day of analysis
596 using the positive calibration solution (Pierce, ThermoFisher Scientific). The ESI source capillary
597 voltage was set to 3.0 kV and the capillary temperature to 275°C. High-resolution full scans were
598 acquired in centroid mode at a resolving power of 30,000 over a mass range of 50 – 1000 *m/z*.
599 Fragmentation data (MS²) were also collected using collision-induced dissociation (CID, He_(g))
600 and a data-dependent acquisition approach on the top 5 most abundant ions in each MS¹ full scan.
601 High-resolution (15,000 resolving power) MS² spectra were collected using a 2 *m/z* precursor
602 isolation width, and an optimized 30% normalized CID energy for fragmentation. Raw LC/MS
603 data were analyzed using the Thermo XCalibur Qual Software. Integrated LC peak areas were
604 obtained from the extracted ion chromatograms (10 ppm tolerance).

605 Accession Numbers and Data Availability

606 Mass spectrometry data was uploaded to the Center for Computation Mass Spectrometry (UCSD)
607 online database MassIVE. The MassIVE ID number is MSV000082488. Microbial 16S rRNA
608 gene amplicon sequences for both DBNPA treated microcosm and the glutaraldehyde treated
609 microcosms were deposited in NCBI Sequence Read Archive (SRA) in SRA accession
610 SRP151211 under BioProject PRJNA476929 as Biosamples SAMN09459387 to
611 SAMN09459570, and SAMN09475542 to SAMN09475579.

612 ACKNOWLEDGMENTS

613 This research was funded by the Methane Center in the Institute for a Secure and Sustainable
614 Environment (<http://isss.utk.edu/methane/>), the Bredesen Center at the University of Tennessee,
615 and the National Science Foundation CBET awards 1805152 (University of Tennessee), 1804685
616 (Michigan Technological University), and 1805549 (Juniata College).

617 SUPPORTING INFORMATION

- 618 Figure S1: DBNPA and known degradation products.
- 619 Figure S2: Microbial Community Shifts Over Time. A) Phylum, B) Genus
- 620 Figure S3: Biotic and abiotic degradation of DBNPA over time. Data is shown averaged by HF+
621 and HF-.
- 622 Figure S4: Biotic and abiotic DBNPA degradation over time. Data is shown by water source
623 location.
- 624 Figure S5: High-resolution mass spectrum of DBNPA standard.
- 625 Figure S6: Number of brominated species detected by nano-HPLC-HRMS in two HF- (left) and
626 two HF+ (right) sets of microcosm samples, biotic and abiotic, from days 0, 7, 14, 21, and 28.
- 627 Figure S7: Summed peak areas for all brominated compounds at each time point (0, 7, 14, and 28
628 days), normalized to each sample set (stream), analyzed by nano-HPLC-HRMS.
- 629 Table S1: DESeq2 results, OTU enrichment 7 days after glutaraldehyde addition
- 630 Table S2: DESeq2 results HF- vs HF+ enrichment at day 7
- 631 Table S3: DESeq2 results, enriched OTU at day 21 vs 0
- 632 Table S4: DESeq2 results, enriched OTU at day 35 vs 0
- 633 Table S5: DESeq2 results, enriched OTU at day 49 vs 0
- 634 Table S6: DESeq2 results, enriched OTU at day 56 vs 0
- 635 Table S7: DESeq2 results HF- vs HF+ enrichment at day 21
- 636 Table S8: DESeq2 results HF- vs HF+ enrichment at day 35
- 637 Table S9: DESeq2 results HF- vs HF+ enrichment at day 49
- 638 Table S10: DESeq2 results HF- vs HF+ enrichment at day 56
- 639 Table S11: DESeq2 results day 56 no-GA vs no-GA
- 640 Table S12: DESeq2 results day 56 vs day 56 no-DBNPA
- 641 Table S13: Putative DBNPA brominated degradation products detected by nano-HPLC-HRMS.
- 642 Table S14: Total Organic Carbon (TOC) concentration in source water prior to DBNPA addition.
- 643 Table S15: Geological coordinates and watershed physiochemical parameters.

644

645 **REFERENCES**

646

- 647 1. EIA US. 2017. Annual Energy Outlook 2017 with Projections to 2035, on U.S.
648 Department of Energy, Energy Information Administration.
649 [https://www.eia.gov/outlooks/aeo/pdf/0383\(2017\).pdf](https://www.eia.gov/outlooks/aeo/pdf/0383(2017).pdf). Accessed
- 650 2. Kahrilas GA, Blotevogel J, Stewart PS, Borch T. 2014. Biocides in hydraulic
651 fracturing fluids: A critical review of their usage, mobility, degradation, and
652 toxicity. *Environ Sci Technol* 49:16-32.
- 653 3. Struchtemeyer CG, Elshahed MS. 2012. Bacterial communities associated
654 with hydraulic fracturing fluids in thermogenic natural gas wells in North
655 Central Texas, USA. *FEMS Microbiology Ecology* 81:13-25.
- 656 4. Muyzer G, Stams AJM. 2008. The ecology and biotechnology of sulphate-
657 reducing bacteria. *Nature Reviews Microbiology* 6:441-454.
- 658 5. Kahrilas GA, Blotevogel J, Corrin ER, Borch T. 2016. Downhole
659 Transformation of the Hydraulic Fracturing Fluid Biocide Glutaraldehyde:
660 Implications for Flowback and Produced Water Quality. *Environ Sci Technol*
661 50:11414-11423.
- 662 6. Stringfellow WT, Domen JK, Camarillo MK, Sandelin WL, Borglin S. 2014.
663 Physical, chemical, and biological characteristics of compounds used in
664 hydraulic fracturing. *Journal of hazardous materials* 275:37-54.
- 665 7. Williams TM, McGinley HR. 2010. Deactivation Of Industrial Water
666 Treatment Biocides, abstr CORROSION 2010, San Antonio, Texas, 2010/1/1/.
667 NACE International, NACE.
- 668 8. Paulus W. 2005. Directory of microbicides for the protection of materials: a
669 handbook. Springer Science & Business Media.
- 670 9. Wolf PA, Sterner PW. 1972. 2,2-dibromo-3-nitrilopropionamide, a compound
671 with slimicidal activity. *Appl Microbiol* 24:581-4.
- 672 10. EPA US. 1994. Reregistration Eligibility Decision (RED) 2,2,-dibromo-3-
673 nitrilopropionamide (DBNPA).
674 <https://archive.epa.gov/pesticides/reregistration/web/pdf/3056.pdf>.
- 675 11. Trexler R, Solomon C, Brislawn CJ, Wright JR, Rosenberger A, McClure EE,
676 Grube AM, Peterson MP, Keddache M, Mason OU, Hazen TC, Grant CJ,
677 Lamendella R. 2014. Assessing impacts of unconventional natural gas
678 extraction on microbial communities in headwater stream ecosystems in
679 Northwestern Pennsylvania. *Frontiers in Microbiology* 5:522.
- 680 12. Ulrich N, Kirchner V, Drucker R, Wright JR, McLimans CJ, Hazen TC, Campa
681 MF, Grant CJ, Lamendella R. 2018. Response of Aquatic Bacterial
682 Communities to Hydraulic Fracturing in Northwestern Pennsylvania: A Five-
683 Year Study. *Scientific Reports* 8:5683.
- 684 13. Blanchard FA, Gonsior SJ, Hopkins DL. 1987. 2,2-Dibromo-3-
685 nitrilopropionamide (DBNPA) chemical degradation in natural waters:

- 686 Experimental evaluation and modeling of competitive pathways. *Water*
687 *Research* 21:801-807.
- 688 14. Richardson SD. 2003. Disinfection by-products and other emerging
689 contaminants in drinking water. *TrAC Trends in Analytical Chemistry*
690 22:666-684.
- 691 15. Exner JH, Burk GA, Kyriacou D. 1973. Rates and Products of Decomposition of
692 2,2-Dibromo-3-Nitrilopropionamide. *Journal of Agricultural and Food*
693 *Chemistry* 21:838-842.
- 694 16. Grant CJ, Weimer AB, Marks NK, Perow ES, Oster JM, Brubaker KM, Trexler
695 RV, Solomon CM, Lamendella R. 2015. Marcellus and mercury: Assessing
696 potential impacts of unconventional natural gas extraction on aquatic
697 ecosystems in northwestern Pennsylvania. *J Environ Sci Health A Tox Hazard*
698 *Subst Environ Eng* 50:482-500.
- 699 17. EPA US. 2012. Study of the potential impacts of hydraulic fracturing on
700 drinking water resources. Agency USEP,
701 [https://www.epa.gov/sites/production/files/documents/hf-](https://www.epa.gov/sites/production/files/documents/hf-report20121214.pdf)
702 [report20121214.pdf](https://www.epa.gov/sites/production/files/documents/hf-report20121214.pdf).
- 703 18. Gross SA, Avens HJ, Banducci AM, Sahmel J, Panko JM, Tvermoes BE. 2013.
704 Analysis of BTEX groundwater concentrations from surface spills associated
705 with hydraulic fracturing operations. *Journal of the Air & Waste Management*
706 *Association* 63:424-432.
- 707 19. Drollette BD, Hoelzer K, Warner NR, Darrah TH, Karatum O, O'Connor MP,
708 Nelson RK, Fernandez LA, Reddy CM, Vengosh A, Jackson RB, Elsner M, Plata
709 DL. 2015. Elevated levels of diesel range organic compounds in groundwater
710 near Marcellus gas operations are derived from surface activities.
711 *Proceedings of the National Academy of Sciences* 112:13184-13189.
- 712 20. Hildenbrand ZL, Carlton DD, Fontenot BE, Meik JM, Walton JL, Taylor JT,
713 Thacker JB, Korlie S, Shelor CP, Henderson D, Kadjo AF, Roelke CE, Hudak PF,
714 Burton T, Rifai HS, Schug KA. 2015. A Comprehensive Analysis of
715 Groundwater Quality in The Barnett Shale Region. *Environ Sci Technol*
716 49:8254-8262.
- 717 21. Akob DM, Mumford AC, Orem W, Engle MA, Klings JG, Kent DB, Cozzarelli
718 IM. 2016. Wastewater Disposal from Unconventional Oil and Gas
719 Development Degrades Stream Quality at a West Virginia Injection Facility.
720 *Environ Sci Technol* 50:5517-5525.
- 721 22. Orem W, Varonka M, Crosby L, Haase K, Loftin K, Hladik M, Akob DM, Tatu C,
722 Mumford A, Jaeschke J, Bates A, Schell T, Cozzarelli I. 2017. Organic
723 geochemistry and toxicology of a stream impacted by unconventional oil and
724 gas wastewater disposal operations. *Applied Geochemistry* 80:155-167.
- 725 23. Shade A, Peter H, Allison SD, Baho DL, Berga M, Burgmann H, Huber DH,
726 Langenheder S, Lennon JT, Martiny JB, Matulich KL, Schmidt TM, Handelsman
727 J. 2012. Fundamentals of microbial community resistance and resilience.
728 *Front Microbiol* 3:417.
- 729 24. Dow. n.d. Delivering Value with an Optimized Microbial Control Program in
730 Oil and Gas Operations.
731 http://msdssearch.dow.com/PublishedLiteratureDOWCOM/dh_097e/0901b

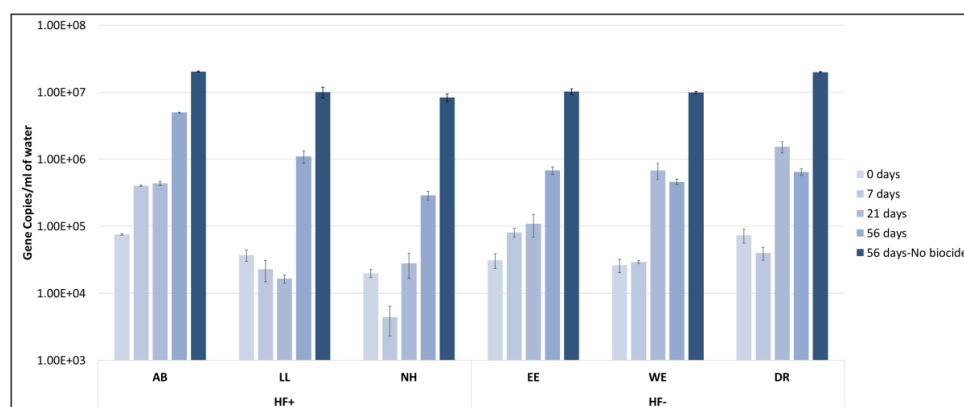
- 732 [8038097eef2.pdf?filepath=microbial/pdfs/noreg/253-](#)
733 [02697.pdf&fromPage=GetDoc](#). Accessed April 30.
- 734 25. Findlay S. 2010. Stream microbial ecology. *Journal of the North American*
735 *Benthological Society* 29:170-181.
- 736 26. Zeglin LH. 2015. Stream microbial diversity in response to environmental
737 changes: review and synthesis of existing research. *Front Microbiol* 6:454.
- 738 27. Smith MB, Rocha AM, Smillie CS, Olesen SW, Paradis C, Wu LY, Campbell JH,
739 Fortney JL, Mehlhorn TL, Lowe KA, Earles JE, Phillips J, Techtman SM, Joyner
740 DC, Elias DA, Bailey KL, Hurt RA, Preheim SP, Sanders MC, Yang J, Mueller MA,
741 Brooks S, Watson DB, Zhang P, He ZL, Dubinsky EA, Adams PD, Arkin AP,
742 Fields MW, Zhou JZ, Alm EJ, Hazen TC. 2015. Natural Bacterial Communities
743 Serve as Quantitative Geochemical Biosensors. *Mbio* 6.
- 744 28. Campa MF, Techtman SM, Gibson CM, Zhu X, Patterson M, Garcia de Matos
745 Amaral A, Ulrich N, Campagna SR, Grant CJ, Lamendella R, Hazen TC. 2018.
746 Impacts of Glutaraldehyde on Microbial Community Structure and
747 Degradation Potential in Streams Impacted by Hydraulic Fracturing. *Environ*
748 *Sci Technol* 52:5989-5999.
- 749 29. Moeseneder MM, Arrieta JM, Herndl GJ. 2005. A comparison of DNA- and
750 RNA-based clone libraries from the same marine bacterioplankton
751 community. *FEMS Microbiol Ecol* 51:341-52.
- 752 30. Hazen TC. 2018. Cometabolic Bioremediation. Consequences of Microbial
753 Interactions with Hydrocarbons, Oils, and Lipids. *In* Steffan R (ed),
754 Biodegradation and Bioremediation doi:[https://doi.org/10.1007/978-3-](https://doi.org/10.1007/978-3-319-44535-9_5-1)
755 [319-44535-9 5-1](https://doi.org/10.1007/978-3-319-44535-9_5-1). Springer International Publishing AG.
- 756 31. Swan BK, Martinez-Garcia M, Preston CM, Sczyrba A, Woyke T, Lamy D,
757 Reinthaler T, Poulton NJ, Masland EDP, Gomez ML, Sieracki ME, DeLong EF,
758 Herndl GJ, Stepanauskas R. 2011. Potential for Chemolithoautotrophy Among
759 Ubiquitous Bacteria Lineages in the Dark Ocean. *Science* 333:1296-1300.
- 760 32. Sanford RA, Chowdhary J, Löffler FE. Organohalide-Respiring
761 *Deltaproteobacteria*. *In* Adrian L, Loeffler FE (ed), Organohalide-Respiring
762 Bacteria doi:10.1007/978-3-662-49875-0. Springer.
- 763 33. Kostka JE, Prakash O, Overholt WA, Green SJ, Freyer G, Canion A, Delgardio J,
764 Norton N, Hazen TC, Huettel M. 2011. Hydrocarbon-Degrading Bacteria and
765 the Bacterial Community Response in Gulf of Mexico Beach Sands Impacted
766 by the Deepwater Horizon Oil Spill. *Applied and Environmental Microbiology*
767 77:7962-7974.
- 768 34. Levy SB. 2002. Active efflux, a common mechanism for biocide and antibiotic
769 resistance. *J Appl Microbiol* 92 Suppl:65S-71S.
- 770 35. Poole K. 2007. Efflux pumps as antimicrobial resistance mechanisms. *Annals*
771 *of Medicine* 39:162-176.
- 772 36. Vikram A, Bomberger JM, Bibby KJ. 2015. Efflux as a Glutaraldehyde
773 Resistance Mechanism in *Pseudomonas fluorescens* and *Pseudomonas*
774 *aeruginosa* Biofilms. *Antimicrobial Agents and Chemotherapy* 59:3433-3440.
- 775 37. Vikram A, Lipus D, Bibby K. 2014. Produced water exposure alters bacterial
776 response to biocides. *Environ Sci Technol* 48:13001-13009.

- 777 38. Comte J, Lindström ES, Eiler A, Langenheder S. 2014. Can marine bacteria be
778 recruited from freshwater sources and the air? *The ISME Journal* 8:2423-
779 2430.
- 780 39. Mumford AC, Akob DM, Klimes JG, Cozzarelli IM. 2018. Common hydraulic
781 fracturing fluid additives alter the structure and function of anaerobic
782 microbial communities. *Applied and Environmental Microbiology*.
- 783 40. Chen See JR, Ulrich N, Nwanosike H, McLimans CJ, Tokarev V, Wright JR,
784 Campa MF, Grant CJ, Hazen TC, Niles JM, Ressler D, Lamendella R. 2018.
785 Bacterial Biomarkers of Marcellus Shale Activity in Pennsylvania. *Frontiers in*
786 *Microbiology* 9.
- 787 41. Mouser PJ, Borton M, Darrah TH, Hartsock A, Wrighton KC. 2016. Hydraulic
788 fracturing offers view of microbial life in the deep terrestrial subsurface.
789 *FEMS Microbiology Ecology* doi:10.1093/femsec/fiw166.
- 790 42. Zhang XX, Zhang T, Fang HH. 2009. Antibiotic resistance genes in water
791 environment. *Appl Microbiol Biotechnol* 82:397-414.
- 792 43. Russell AD. 2001. Mechanisms of bacterial insusceptibility to biocides. *Am J*
793 *Infect Control* 29:259-61.
- 794 44. Setlow P. 2006. Spores of *Bacillus subtilis*: their resistance to and killing by
795 radiation, heat and chemicals. *J Appl Microbiol* 101:514-25.
- 796 45. Furuhashi K, Kato Y, Goto K, Hara M, Yoshida S-i, Fukuyama M. 2006. Isolation
797 and Identification of *Methylobacterium* Species from the Tap Water in
798 Hospitals in Japan and Their Antibiotic Susceptibility. *Microbiology and*
799 *Immunology* 50:11-17.
- 800 46. Gan HM, Hudson AO, Rahman AYA, Chan KG, Savka MA. 2013. Comparative
801 genomic analysis of six bacteria belonging to the genus *Novosphingobium*:
802 insights into marine adaptation, cell-cell signaling and bioremediation. *BMC*
803 *genomics* 14:431-431.
- 804 47. Vikram A, Lipus D, Bibby K. 2016. Metatranscriptome analysis of active
805 microbial communities in produced water samples from the Marcellus Shale.
806 *Microb Ecol* 72:571-81.
- 807 48. Rogers JD, Ferrer I, Tummings SS, Bielefeldt AR, Ryan JN. 2017. Inhibition of
808 Biodegradation of Hydraulic Fracturing Compounds by Glutaraldehyde:
809 Groundwater Column and Microcosm Experiments. *Environ Sci Technol*
810 51:10251-10261.
- 811 49. McLaughlin MC, Borch T, Blotvogel J. 2016. Spills of Hydraulic Fracturing
812 Chemicals on Agricultural Topsoil: Biodegradation, Sorption, and Co-
813 contaminant Interactions. *Environ Sci Technol* 50:6071-8.
- 814 50. Matzek LW, Carter KE. 2017. Sustained persulfate activation using solid iron:
815 Kinetics and application to ciprofloxacin degradation. *Chemical Engineering*
816 *Journal* 307:650-660.
- 817 51. McDonnell G, Russell AD. 1999. Antiseptics and disinfectants: activity, action,
818 and resistance. *Clin Microbiol Rev* 12:147-79.
- 819 52. Villanueva CM, Cordier S, Font-Ribera L, Salas LA, Levallois P. 2015. Overview
820 of Disinfection By-products and Associated Health Effects. *Current*
821 *Environmental Health Reports* 2:107-115.

- 822 53. Li X-F, Mitch WA. 2018. Drinking Water Disinfection Byproducts (DBPs) and
823 Human Health Effects: Multidisciplinary Challenges and Opportunities.
824 Environ Sci Technol 52:1681-1689.
- 825 54. Hladik ML, Focazio MJ, Engle M. 2014. Discharges of produced waters from
826 oil and gas extraction via wastewater treatment plants are sources of
827 disinfection by-products to receiving streams. Science of The Total
828 Environment 466-467:1085-1093.
- 829 55. Akyon B, McLaughlin M, Hernández F, Blotevogel J, Bibby K. 2019.
830 Characterization and biological removal of organic compounds from
831 hydraulic fracturing produced water. Environmental Science: Processes &
832 Impacts.
- 833 56. Grant CJ, Lutz AK, Kulig AD, Stanton MR. 2016. Fracked ecology: Response of
834 aquatic trophic structure and mercury biomagnification dynamics in the
835 Marcellus Shale Formation. Ecotoxicology 25:1739-1750.
- 836 57. Janssen DB, Oppentocht JE, Poelarends GJ. 2001. Microbial dehalogenation.
837 Curr Opin Biotechnol 12:254-8.
- 838 58. Mohn WW, Tiedje JM. 1992. Microbial reductive dehalogenation. Microbiol
839 Rev 56:482-507.
- 840 59. Fetzner S, Lingens F. 1994. Bacterial dehalogenases: biochemistry, genetics,
841 and biotechnological applications. Microbiol Rev 58:641-85.
- 842 60. Levis E. 2016. Texas Company Pays \$93,710 settlement for polluting
843 Clearfield County Creek. Pennsylvania Fish and Boat Commision., p *In*
844 Pennsylvania Fish and Boat Commision. Harrisburg, PA.
845 [https://hero.epa.gov/hero/index.cfm/reference/details/reference_id/24478](https://hero.epa.gov/hero/index.cfm/reference/details/reference_id/2447894)
846 [94](https://hero.epa.gov/hero/index.cfm/reference/details/reference_id/2447894).
- 847 61. PADEP. 2013. Oil and Gas Annual Report. Pennsylvania Department of
848 Environmental Protection Office of Oil and Gas Management,
- 849 62. Dunlap K. 2011. Shale gas production and water resources in the eastern
850 United States, *on* U.S. Senate Committee on Energy and Natural Resources
851 Subcommittee on Water and Power.
852 [https://www.energy.senate.gov/public/index.cfm/files/serve?File_id=1CBE](https://www.energy.senate.gov/public/index.cfm/files/serve?File_id=1CBE5C49-AA41-4BEC-A6B7-992068C59666)
853 [5C49-AA41-4BEC-A6B7-992068C59666](https://www.energy.senate.gov/public/index.cfm/files/serve?File_id=1CBE5C49-AA41-4BEC-A6B7-992068C59666). Accessed April 1, 2018.
- 854 63. Lutz AK, Grant CJ. 2016. Impacts of hydraulic fracturing development on
855 macroinvertebrate biodiversity and gill morphology of net-spinning caddisfly
856 (Hydropsychidae, Diplectrona) in northwestern Pennsylvania, USA. Journal
857 of Freshwater Ecology 31:211-217.
- 858 64. Caporaso JG, Kuczynski J, Stombaugh J, Bittinger K, Bushman FD, Costello EK,
859 Fierer N, Pena AG, Goodrich JK, Gordon JL, Huttley GA, Kelley ST, Knights D,
860 Koenig JE, Ley RE, Lozupone CA, McDonald D, Muegge BD, Pirrung M, Reeder
861 J, Sevinsky JR, Turnbaugh PJ, Walters WA, Widmann J, Yatsunenko T,
862 Zaneveld J, Knight R. 2010. QIIME allows analysis of high-throughput
863 community sequencing data. Nat Methods 7:335-6.
- 864 65. Edgar RC. 2010. Search and clustering orders of magnitude faster than
865 BLAST. Bioinformatics 26:2460-1.
- 866 66. Edgar RC, Haas BJ, Clemente JC, Quince C, Knight R. 2011. UCHIME improves
867 sensitivity and speed of chimera detection. Bioinformatics 27:2194-200.

- 868 67. DeSantis TZ, Hugenholtz P, Larsen N, Rojas M, Brodie EL, Keller K, Huber T,
869 Dalevi D, Hu P, Andersen GL. 2006. Greengenes, a chimera-checked 16S rRNA
870 gene database and workbench compatible with ARB. *Appl Environ Microbiol*
871 72:5069-72.
- 872 68. Caporaso JG, Bittinger K, Bushman FD, DeSantis TZ, Andersen GL, Knight R.
873 2010. PyNAST: a flexible tool for aligning sequences to a template alignment.
874 *Bioinformatics* 26:266-7.
- 875 69. Wang Q, Garrity GM, Tiedje JM, Cole JR. 2007. Naive Bayesian classifier for
876 rapid assignment of rRNA sequences into the new bacterial taxonomy. *Appl*
877 *Environ Microbiol* 73:5261-7.
- 878 70. Paulson JN, Stine OC, Bravo HC, Pop M. 2013. Differential abundance analysis
879 for microbial marker-gene surveys. *Nature Methods* 10:1200.
- 880 71. Lozupone C, Lladser ME, Knights D, Stombaugh J, Knight R. 2011. UniFrac: an
881 effective distance metric for microbial community comparison. *The ISME*
882 *journal* 5:169-172.
- 883 72. Vázquez-Baeza Y, Pirrung M, Gonzalez A, Knight R. 2013. EMPeror: a tool for
884 visualizing high-throughput microbial community data. *GigaScience* 2:16-16.
- 885 73. McMurdie PJ, Holmes S. 2013. phyloseq: an R package for reproducible
886 interactive analysis and graphics of microbiome census data. *PLoS One*
887 8:e61217.
- 888 74. Dixon P. 2003. VEGAN, a package of R functions for community ecology.
889 *Journal of Vegetation Science* 14:927-930.
- 890 75. McMurdie PJ, Holmes S. 2014. Waste not, want not: why rarefying
891 microbiome data is inadmissible. *PLoS computational biology* 10:e1003531-
892 e1003531.
- 893 76. Love MI, Huber W, Anders S. 2014. Moderated estimation of fold change and
894 dispersion for RNA-seq data with DESeq2. *Genome Biol* 15:550.
- 895 77. Pinheiro JB, D.; DebRoy, S.; Sarkar, D.; and R Core Team 2018. nlme: Linear
896 and Nonlinear Mixed Effects Models. R package version 31-1311.
- 897 78. Lenth RL, J.; Herve, M. 2018. Estimated Marginal Means, aka Least-Square
898 Means. R package version 112.
- 899

900 **FIGURES AND LEGENDS**



901

902 **Figure 1.** Impacts of DBNPA in abundance of 16S rRNA gene copies/mL over time. Data shown

903 is divided by HF-impacted (first three clusters, Alex Branch (AB), Little Laurel (LL), Naval

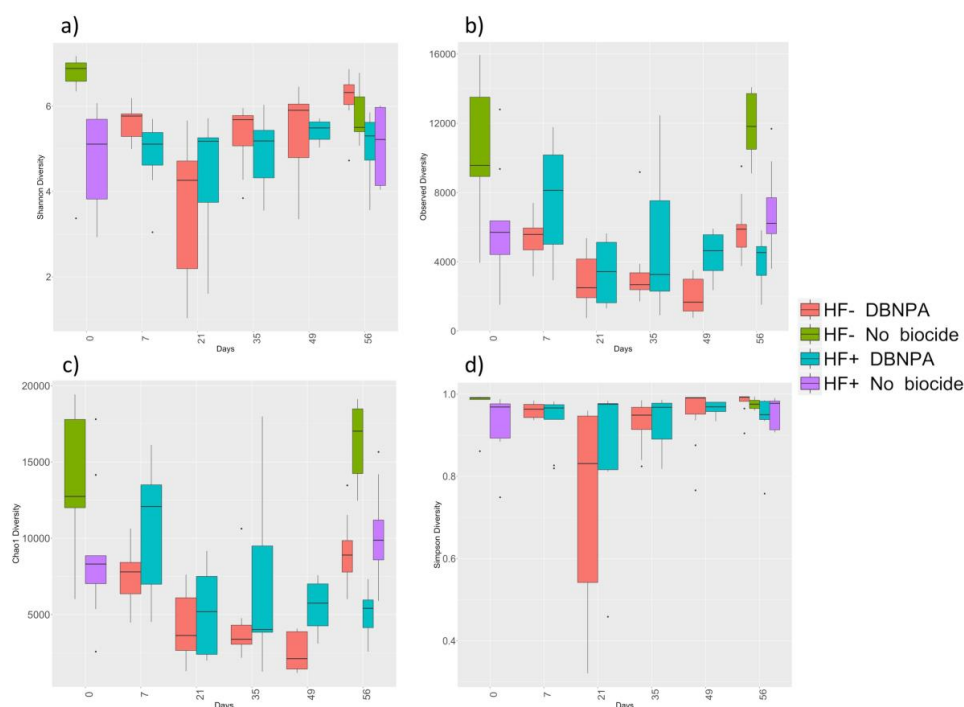
904 Hollow (NH)) and HF-unimpacted (East Elk (EE), West Elk (WE), Dixon Run (DR))

905 microcosms at day zero before DBNPA addition, day 7, 21, and 56 after DBNPA addition, and

906 day 56 no-DBNPA added control. The bars are color on a gradient over time, with the last bar

907 representing the no-DBNPA control at day 56. Each bar represents n=3, and the error bars

908 represent one standard error.



909

910 **Figure 2.** Four different richness and evenness alpha diversity estimators comparing HF-

911 impacted and HF-unimpacted microcosms over time. The estimators used were (a) Shannon

912 Diversity, (b) Observed Diversity, (c) Chao1, and (d) Simpson Diversity. Red and green represent

913 HF-unimpacted microcosms. Red boxes represent the changes after DBNPA addition in HF-

914 unimpacted (days 7 to 56), while the green boxes represent the alpha diversity without DBNPA

915 addition in HF- (day zero and 56). Blue and purple boxes represent HF-impacted microcosms.

916 Blue boxes represent the changes after DBNPA addition in HF-impacted (days 7 to 56), while the

917 purple boxes represent the alpha diversity without DBNPA addition in HF- (day zero and 56).

918 The box and whisker plot described the distribution of the data points. The beginning of the

919 whiskers to the beginning of the box are the upper and lower quartiles. The box represents the

920 interquartile range, which represents 50% of the data points (n=9). The vertical line inside the box

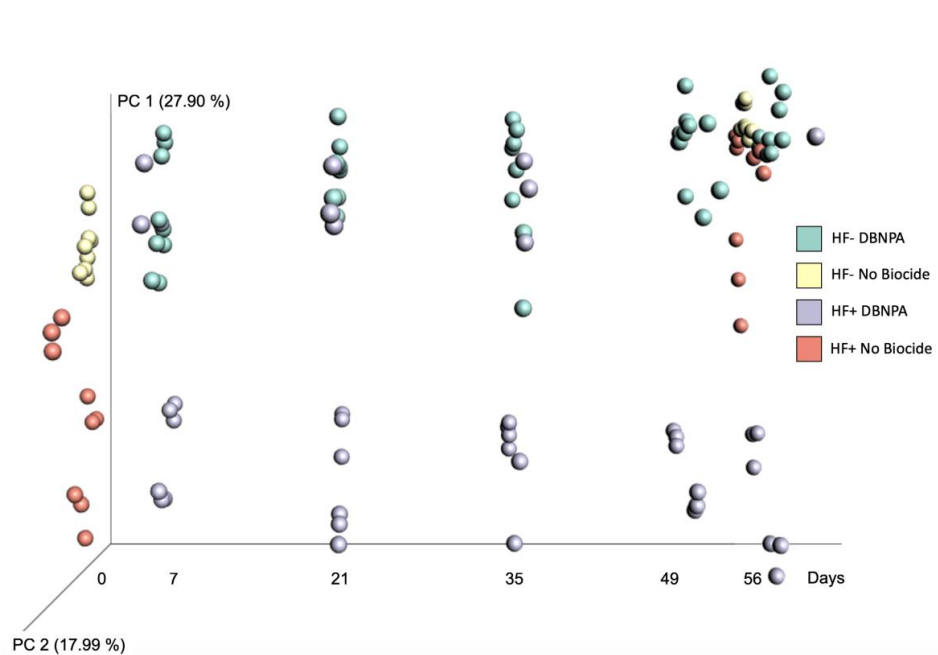
921 represents the median.

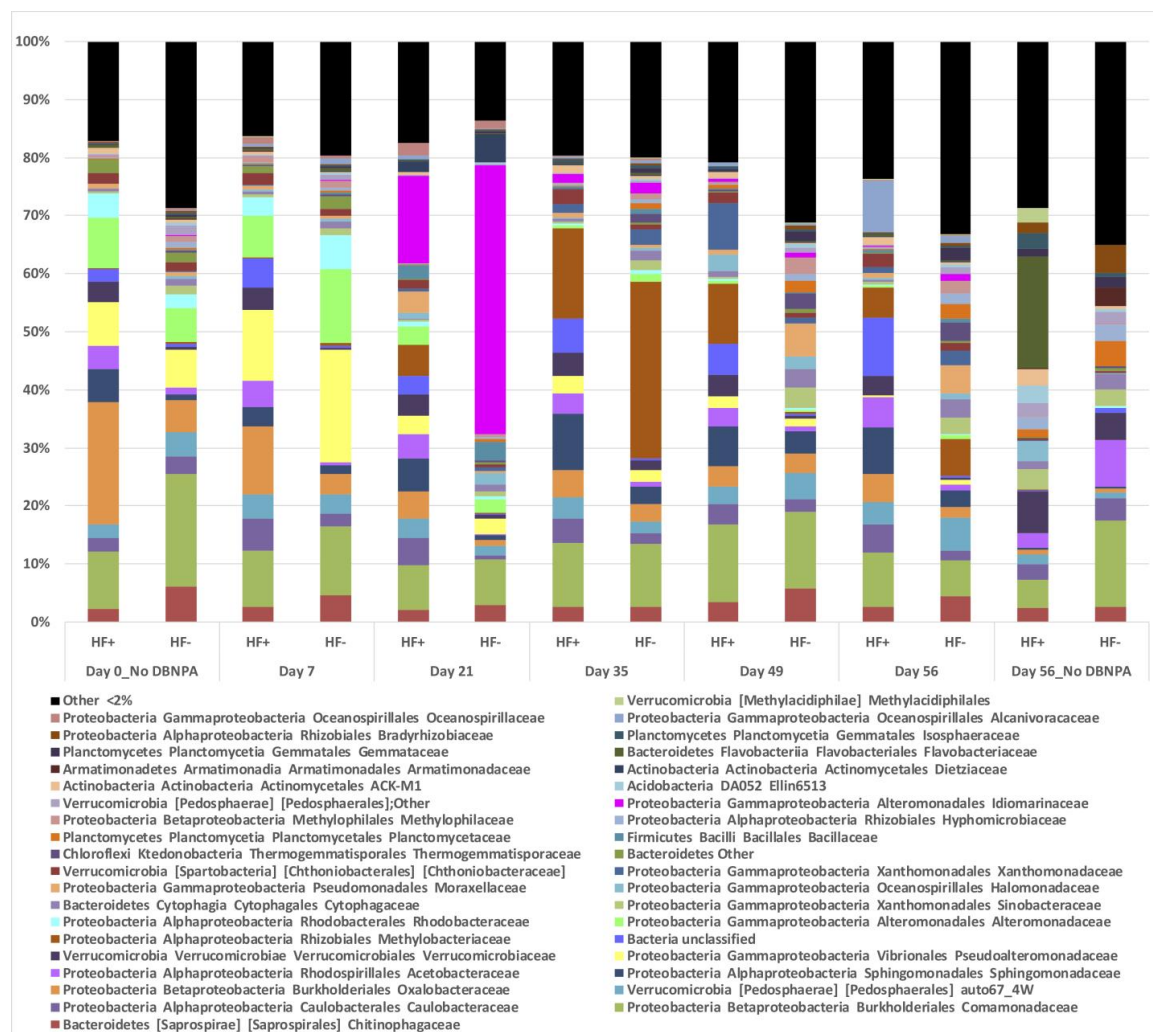
922

923

924 **Figure 3.** Directional Principal Coordinate Analysis (PCoA) plots of weighted UniFrac distances
925 between microcosms. Samples were plotted on the x-axis from left to right according to days
926 sampled, 0, 7, 21, 35, 49, and 56. Samples are colored by hydraulic fracturing (HF)-impact
927 history and DBNPA addition. The green legend = HF-unimpacted plus DBNPA addition, yellow
928 legend= HF-unimpacted without biocide addition, purple legend= HF-impacted plus DBNPA
929 addition, and pink legend= HF-impacted without biocide addition. Samples without biocide
930 addition were only measured day 0 and day 56.

931





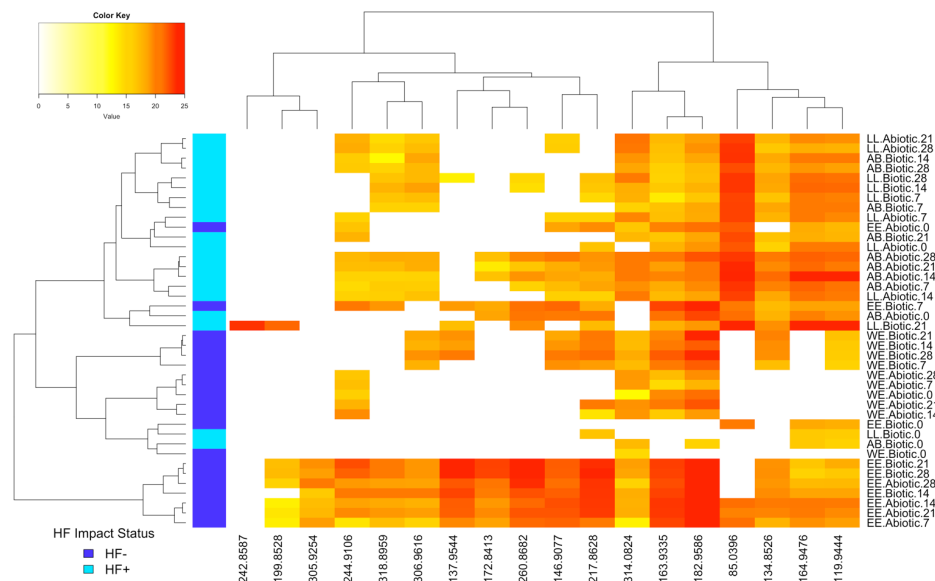
932

933 **Figure 4.** Temporal changes of microbial community relative abundance in averaged hydraulic

934 fracturing-impacted (HF+) and hydraulic fracturing-unimpacted (HF-) microcosms treated with

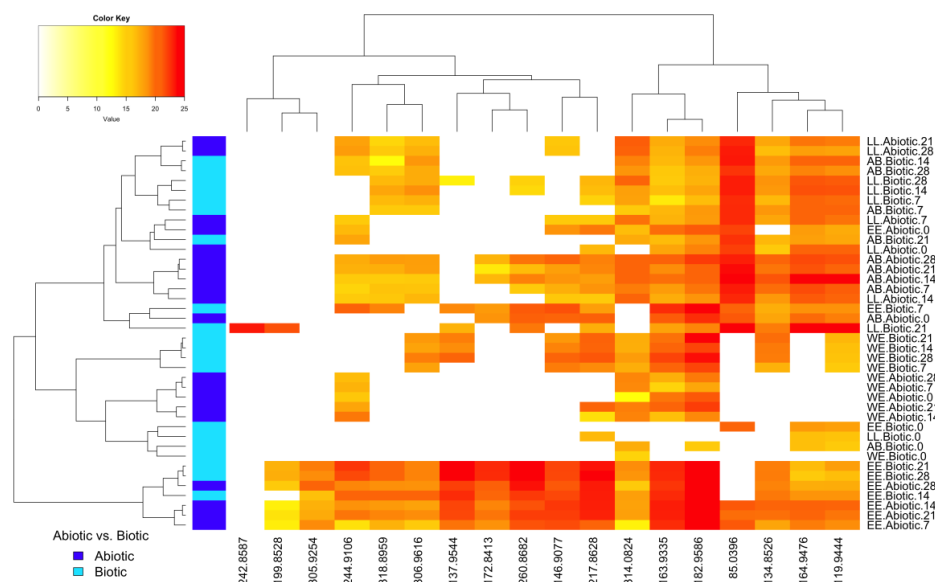
935 the biocide DBNPA. Microbial taxa are summarized to the Family level.

936 A)



937

938 B)



939

940 **Figure 5.** Heat maps of the normalized \log_2 peak areas for brominated species detected by nano-
941 HPLC-HRMS. The dendrograms cluster samples using the Ward method of agglomeration. Rows
942 represent samples (described by stream location, condition, and day of collection) and columns
943 represent m/z ratios of the brominated species detected. The top dendrogram is clustered by
944 brominated species that varied similarly across the data set. A) The left dendrogram clusters first
945 by HF+ (light blue) or HF- (dark blue) streams, and then by abiotic and biotic microcosms. B)
946 The left dendrogram clusters by abiotic (dark blue) and biotic (light blue) samples.
947

948 **Table 1.** Nested PERMANOVA of weighted UniFrac distances
949

Source of Variation	Degrees of Freedom	Sum of Squares	Mean Square	F. Model	R2	P value
HF_ImpactStatus	1	0.9515	0.95148	30.3412	0.15771	0.001
Biocide	1	0.4506	0.45056	14.3678	0.07468	0.001
Biocide:Days	2	0.7840	0.39199	12.5000	0.12995	0.001
HF_ImpactStatus: Biocide	1	0.1381	0.13806	4.4024	0.02288	0.001
HF_ImpactStatus: Biocide: Days	2	0.1653	0.08266	2.6359	0.02740	0.001
Residuals	113	3.5436	0.03136		0.58737	
Total	120	6.0330			1.00000	

950

951

952